Determination of Relative $CMRO_2$ From CBF and BOLD Changes: Significant Increase of Oxygen Consumption Rate During Visual Stimulation

Seong-Gi Kim,[1]* Egill Rostrup,[2] Henrik B.W. Larsson,[2] Seiji Ogawa,[3] and Olaf B. Paulson[2]

The blood oxygenation level-dependent (BOLD) effect in functional magnetic resonance imaging depends on at least partial uncoupling between cerebral blood flow (CBF) and cerebral metabolic rate of oxygen ($CMRO_2$) changes. By measuring CBF and BOLD simultaneously, the relative change in $CMRO_2$ can be estimated during neural activity using a reference condition obtained with known $CMRO_2$ change. In this work, nine subjects were studied at a magnetic field of 1.5 T; each subject underwent inhalation of a 5% carbon dioxide gas mixture as a reference and two visual stimulation studies. Relative CBF and BOLD signal changes were measured simultaneously using the flow-sensitive alternating inversion recovery (FAIR) technique. During hypercapnia established by an end-tidal CO_2 increase of 1.46 kPa, CBF in the visual cortex increased by 47.3 ± 17.3% (mean ± SD; $n = 9$), and $\Delta R_2'$ was -0.478 ± 0.147 sec^{-1}, which corresponds to BOLD signal change of 2.4 ± 0.7% with a gradient echo time of 50 msec. During black/white visual stimulation reversing at 8 Hz, regional CBF increase in the visual cortex was 43.6 ± 9.4% ($n = 18$), and $\Delta R_2'$ was -0.114 ± 0.086 sec^{-1}, corresponding to a BOLD signal change of 0.6 ± 0.4%. Assuming that $CMRO_2$ does not change during hypercapnia and that hemodynamic responses during hypercapnia and neural stimulation are similar, relative $CMRO_2$ change was determined using BOLD biophysical models. The average $CMRO_2$ change in the visual cortex ranged from 15.6 ± 8.1% ($n = 18$) with significant cerebral blood volume (CBV) contribution to 29.6 ± 18.8% without significant CBV contribution. A weak positive correlation between CBF and $CMRO_2$ changes was observed, suggesting the $CMRO_2$ increase is proportional to the CBF increase. Magn Reson Med 41:1152–1161, 1999. © **1999 Wiley-Liss, Inc.**

Key words: hypercapnia; perfusion; coupling; oxygen consumption

It is well accepted that during increased neural activity, the cerebral metabolism rate of glucose (CMRglu) is increased and concurrently, cerebral blood flow (CBF) and cerebral blood volume (CBV) are elevated (for review, see ref. 1). CMRglu and CBF increase to a similar extent following neural stimulation (2,3), in agreement with the close coupling between metabolism and CBF. However, the relative change in cerebral metabolic rate of oxygen ($CMRO_2$) during neural activity is still controversial. Two opposite views exist: one (referred to as ''uncoupling'') is that $CMRO_2$ change during neural activity is very small and the other (referred to as ''coupling'') is that $CMRO_2$ increase and CBF/CMRglu change are of similar magnitude. The notion of *uncoupling* between CBF and $CMRO_2$ was reported by Fox et al. (2,3), who found that CBF increased by 50% during neural stimulation, while $CMRO_2$ increased only by 5%. When the CBF increase is higher than the $CMRO_2$ increase, modulation of blood oxygenation level-dependent (BOLD) contrast would be expected due to the excess of diamagnetic oxyhemoglobin concentration in capillaries and venous vessels (4). This phenomenon is the basis of the most commonly used fMRI technique. BOLD signal changes have been observed in various fMRI studies of visual stimulation and performance of other sensory and cognitive tasks (e.g., refs. 5–7), suggesting there is at least partial mismatch between CBF and $CMRO_2$. However, this belief is not universally accepted. Tight *coupling* between CBF and $CMRO_2$ during neural stimulation has been proposed (8). Roland and coworkers (9) observed complete coupling between CBF and $CMRO_2$ in the prefrontal cortex, frontal eye fields, parietal lobe, and thalamus during pure mental activity. Similarly, Marrett et al. (10) reported 25% CBF and 28% $CMRO_2$ increases in the primary visual cortex during red/black reversing circular checkerboard stimulation. As an extreme case, Brodersen et al. (11) found that CBF and $CMRO_2$ increased by 111% and 100%, respectively, during seizure. Recently, Hyder et al. (12) found that $CMRO_2$ measured by ^{1}H spectroscopy increased by 200–400% during forepaw stimulation in rat. To examine these controversial findings regarding the relationship between CBF and $CMRO_2$ changes during neural stimulation, it is necessary to develop a simple MRI method that can be easily repeated and that will faithfully reflect the change in $CMRO_2$.

Since BOLD is related to a mismatch between CBF and $CMRO_2$ increases (13,14), $CMRO_2$ can be calculated from BOLD and CBF measurements (15,16). To calibrate the relationship between BOLD and CBF/$CMRO_2$, hypercapnia (known to provoke an increase in CBF) can be used as a ''control'' reference, assuming that there are no metabolic changes involved in the transition to and from hypercapnia (17–19). An additional underlying assumption is that hemodynamic responses during neural activation and hypercapnia conditions are similar. Then, using hypercapnia studies, oxygen consumption change can be estimated during increased neural activity.

In this paper, we focused on two specific goals; one was to develop a methodology for determining relative $CMRO_2$ change from simultaneously measured CBF and BOLD, and the other was to obtain relative $CMRO_2$ changes during

[1]Center for Magnetic Resonance Research, Department of Radiology, University of Minnesota, Minneapolis, Minnesota.

[2]Danish Research Center for Magnetic Resonance, University of Copenhagen, Hvidovre Hospital, Hvidovre, Denmark.

[3]Bell Laboratories, Lucent Technologies, Murray Hill, New Jersey.

Grant sponsor: NIH Human Brain Projects; Grant number: MH57180; Grant sponsor: NIH Regional Resources; Grant number: RR08079; Grant sponsor: The Whitaker Foundation.

*Correspondence to: Seong-Gi Kim, CMRR, University of Minnesota Medical School, 2021 6th St. SE, Minneapolis, MN 55455. E-mail: kim@cmrr.umn.edu

Received 26 August 1998; revised 15 January 1999; accepted 18 January 1999.

the well-established visual stimulation in humans. We measured CBF and BOLD changes *simultaneously* during hypercapnia and black/white visual stimulation using the flow-sensitive alternating inversion recovery (FAIR) technique (20–23). Hypercapnia conditions in which subjects breathed 5% CO_2 gas mixture were employed to determine the mechanism of BOLD. The $CMRO_2$ change in the visual cortex during visual stimulation was determined from BOLD and CBF changes using a BOLD biophysical model (14).

THEORY

BOLD Biophysical Model

Various theories that assess the BOLD effect in terms of hemodynamic parameters have been presented (13,14). According to these models (13,14), the BOLD signal can be altered by changes in CBV and concentration of blood deoxyhemoglobin; the latter solely depends on CBF and $CMRO_2$. A decrease in venous deoxyhemoglobin concentration increases the BOLD signal intensity, while an increase in CBV decreases the BOLD signal. Since the BOLD signal intensity is proportional to $\exp(-R_2^* \cdot TE)$ where R_2^* ($\equiv 1/T_2^*$) is the apparent transverse relaxation rate induced by local susceptibility effect and TE is the echo time, the BOLD signal increase corresponds to a decrease in R_2^*. Quantitatively, R_2^* induced by local susceptibility effect can be approximated in a given voxel by $R_2^* = \alpha \cdot \nu_{BOLD} \cdot (1 - y)^\beta$, where ν_{BOLD} is the part of the total venous volume fraction *that contributes to the BOLD* signal, y is the venous oxygenation level, and α and β are constants. ν_{BOLD} varies between imaging sequences (such as gradient-echo and spin-echo), imaging parameters, and magnetic fields. α is related to vessel orientation, vessel size, hematocrit level, magnetic field strength (B_0), and the susceptibility difference between completely deoxygenated and completely oxygenated blood (13,14). The power term β is related to vessel size, ranging between 1.0 and 2.0 (13,14).

Transient CBV changes cannot be measured repeatedly using clinically approved contrast agents in humans. However, relative CBF changes can be easily measured using arterial spin tagging techniques (20,24). CBV changes can be obtained from CBF changes by using the relationship between CBF and CBV changes established in monkeys during hypercapnia (25):

$$\frac{\Delta\nu}{\nu} = \left(\frac{\Delta f}{f} + 1\right)^{0.38} - 1 \qquad [1]$$

where $\Delta\nu/\nu$ and $\Delta f/f$ are relative CBV and CBF changes. To examine whether this relationship can be applied to humans during neuronal activity, we relied on previously published positron emission tomography (PET) measurements of CBF and CBV changes during functional activity (2,3). The calculated CBV changes obtained from measured CBF values of 50% during visual stimulation and 29% during somatosensory stimulation using Eq. [1] were 17% and 9%, and they agree well with the experimental data, 16% and 7%, respectively. Thus, we assumed that Eq. [1] can be used to calculate CBV changes during both hypercapnia and neural stimulation. In the case that blood volume changes are not uniform across vessels with different sizes and types, the CBV change related to BOLD signal of a specific MR technique, $\Delta\nu_{BOLD}/\nu_{BOLD}$, is not the same as the $\Delta\nu/\nu$ calculated from Eq. [1]. We assume that the relative increase in blood volume contributing to BOLD, $\Delta\nu_{BOLD}/\nu_{BOLD}$, is proportional to the actual relative increase in blood volume, $\Delta\nu/\nu$, by a constant κ: $\Delta\nu_{BOLD}/\nu_{BOLD} = \kappa \cdot \Delta\nu/\nu$. κ is likely to be less than 1.0 because blood volume increases are higher in arterial vessels than in (BOLD-sensitive) venous vessels.

Defining Δy as the change in venous blood oxygenation level upon neural activation and $\Delta\nu_{BOLD}$ as the change in blood volume upon activation, the apparent relaxation rate during activation is given by $\alpha(\nu_{BOLD} + \Delta\nu_{BOLD})(1 - y - \Delta y)^\beta$. Thus, change in R_2^* upon activation (ΔR_2^*) is given by $\Delta R_2^* = \alpha(\nu_{BOLD} + \Delta\nu_{BOLD})(1 - y - \Delta y)^\beta - \alpha\nu_{BOLD}(1 - y)^\beta$. Since the change in venous blood oxygenation level is relatively small, the term $(1 - y - \Delta y)^\beta$ can be approximated by first-order Taylor expansion: $(1 - y - \Delta y)^\beta \approx (1 - y)^\beta[1 - \beta\Delta y/(1 - y)]$. Since contribution from a multiplication term, $\Delta y/(1 - y)$ times $\Delta\nu_{BOLD}$, is much less than the first-order terms, only first-order terms are included. When ΔR_2^* is small enough, the relative increase in T_2^*-weighted BOLD signal upon activation (ΔBOLD/BOLD) is approximated by $-TE \cdot \Delta R_2^*$. Then, ΔR_2^* is approximately

$$\Delta R_2^* = -\frac{\Delta BOLD}{BOLD} \cdot \frac{1}{TE}$$

$$= -\alpha^* \left\{ \frac{\Delta y}{1 - y} - \frac{1}{\beta} \cdot \frac{\Delta\nu_{BOLD}}{\nu_{BOLD}} \right\} = -\alpha^* \left\{ \frac{\Delta y}{1 - y} - \beta^* \frac{\Delta\nu}{\nu} \right\} \qquad [2]$$

where α^* is $\alpha\beta(1 - y)^\beta\nu_{BOLD}$, and β^* is κ/β. Since α^* is closely related to parameters such as y, α^* is region and subject specific. However, β^* is less variable than α^* because it is only related to vessel size. Regardless of subjects, vessels with similar size will have the same contribution to BOLD when the same imaging sequence is used at a given magnetic field. Thus, β^* is constant across subjects (13,14).

The utilization of O_2 in tissue is the arteriovenous difference of O_2 multiplied by flow, and thus $CMRO_2$ is dependent on CBF $\cdot (1 - y)$ assuming an arterial oxygen saturation of 1.0. Using the conservation of matter, the relative change of $CMRO_2$ in tissue, $\Delta CMRO_2/CMRO_2$, can be determined from the relative changes of both CBF and y in the following manner (14):

$$\frac{\Delta CMRO_2}{CMRO_2} = \left(\frac{\Delta f}{f} + 1\right) \cdot \left(1 - \frac{\Delta y}{1 - y}\right) - 1. \qquad [3]$$

Calculation of $CMRO_2$ Change From BOLD and CBF Data

Figure 1 shows a flow chart used to calculate the constants α^* and β^* of the BOLD biophysical model described above (left column) and to determine $CMRO_2$ change during neural stimulation using these constants (right column). Numbers inside circles represent steps for determining $\Delta CMRO_2/CMRO_2$. From constants obtained under hypercapnic conditions (steps 1–3), $\Delta CMRO_2/CMRO_2$ can be determined from simultaneously obtained BOLD and CBF values during neural stimulation, using biophysical mod-

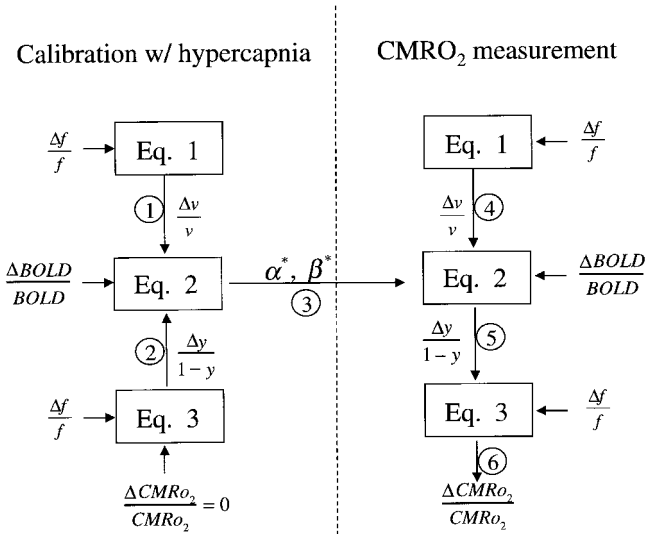

FIG. 1. Scheme to calculate calibration constants (α* and β*) using a hypercapnia model and to determine relative $CMRO_2$ changes ($\Delta CMRO_2/CMRO_2$) during mental activity. $\Delta f/f$ represents relative CBF change; ΔBOLD/BOLD, relative BOLD change; $\Delta v/v$, relative CBV change; and $\Delta y/(1-y)$, relative venous oxygenation level change. Arrows indicate directions of each calculation step. Numbers inside circles represent steps for determining $\Delta CMRO_2/CMRO_2$.

els (steps 4–6). The underlying assumptions of this methodology are the following:

1. A major physiological source of BOLD is the susceptibility change induced by venous oxygenation level and CBV modulations.
2. $CMRO_2$ does not change during hypercapnia.
3. Relationships between CBF and CBV changes during hypercapnia and neural stimulation are similar.

To calculate the constants α* and β* from hypercapnia, two measurements are needed. We previously measured global CBF increases and ΔBOLD/BOLD during inhalation of 5% and 7% CO_2 gas mixtures (26). The CBF changes were 58% and 108%, while the corresponding ΔBOLD/BOLD were 4.96% and 8.59% in the cortical gray matter and 3.24% and 4.80% in the central gray matter with a TE of 60 msec. $\Delta v/v$ calculated from Eq. [1] were 0.19 and 0.32 (step 1). $\Delta y/(1-y)$ values calculated using Eq. [3] were 0.37 and 0.52 (step 2). Constants α* and β* were determined using Eq. [2] (step 3); values of α* were 1.76 and 1.55 sec^{-1}, and those of β* were −0.07 and 0.01 for cortical and central gray matter areas, respectively. Therefore we assumed that β* = 0.0, and α* was determined for each individual subject (referred to as Model 1). Since determinations of calibration constants and consequently $\Delta CMRO_2/CMRO_2$ are closely dependent on the biophysical model used, $\Delta CMRO_2/CMRO_2$ was also calculated by assuming β* = 1.0 (referred to as Model 2) (27). In this model, a higher oxygenation level (and consequently lower oxygen consumption rate change) than in Model 1 are required to have the same magnitude of BOLD change. Therefore, Model 2 gives a lower estimate of magnitude change in oxygen consumption rate. Since we assumed that β* equals either 1.0 or 0.0, only a single hypercapnia condition is needed in order to calculate α*.

To calculate $\Delta CMRO_2/CMRO_2$ with the obtained constants, a straightforward approach was adopted. Initially, Eq. [1] was used to calculate $\Delta v/v$ from $\Delta f/f$ using data obtained during neural stimulation (step 4). Then, $\Delta y/(1-y)$ was determined from BOLD and $\Delta v/v$, α* and β* using Eq. [2] (step 5). Finally, the change in oxygen consumption rate was calculated directly using Eq. [3] (step 6).

MATERIALS AND METHODS

MRI Studies

Nine normal subjects (24.4 ± 1.9 years old, six men and 3 women) were studied on a Siemens 1.5 T Vision system with a homogenous head coil. This protocol was approved by the local ethical committee. A 1-cm-thick oblique imaging slice was selected along the calcarine fissure to cover the primary visual cortex. As described previously (15,20,21,28), the FAIR technique was used to detect CBF and BOLD signal changes simultaneously. Typical imaging parameters were a matrix size of 64 × 64, a field of view of 23 × 23 cm^2, slice thickness of 1 cm, inversion slab of 1.9 cm, TI of 1.4 sec, TE of 50 msec, and TR of 3.16 sec. The temporal resolution was 6.32 sec. Every subject performed one hypercapnia and two visual stimulation studies.

For hypercapnia studies, a gas mixture with 5% CO_2, 21% O_2, and 74% N_2 was used. FAIR images were acquired initially during inhalation of normal atmospheric air, then during inhalation of the CO_2 gas mixture, and finally during inhalation of atmospheric air. At each condition, 40–43 images were acquired. End-tidal CO_2 levels (pCO_2) were measured continuously using a capnometer (Ohmeda, model #4700). Experimental details were previously described (26).

For each fMRI study, four control and four stimulation periods were alternated. In each period, 10 images were acquired. Visual stimulation consisted of a circular black and white checkerboard, reversing at 8 Hz. A small fixation dot was used during whole fMRI studies. Typically two studies were performed during inhalation of atmospheric air; one before and one after hypercapnia.

Data Analysis

Images of 64 × 64 matrix size were interpolated to 128 × 128. FAIR images were obtained from subtraction of non-slice-selective IR images from slice-selective IR images (15,20,21,28). Since we used echoplanar imaging (EPI) for data collection, the BOLD effect contributes to both slice-selective and non-slice-selective IR images (15,20,21,28). BOLD change was obtained from non-slice-selective IR images. Relative CBF change was calculated by taking into account the BOLD effect: $\Delta f/f$ = (1 + fractional signal change of FAIR)/(1 + fraction signal change of BOLD) − 1. Head motion was corrected using an automatic image registration algorithm (29).

Functional maps were calculated using a boxcar cross correlation method (30) with a cross-correlation threshold of 0.3 in the STIMULATE program. Regions with less than eight contiguous active pixels were not included (31) because of interpolation. Since multiple comparisons were performed, modified Bonferroni correction was performed with a cross-correlation value of 0.3, an image number of

80, and a minimal cluster size of 8 (32); a corresponding *P* value is less than 1.1×10^{-6}. In each subject, a region of interest (ROI) was chosen from active pixels within the visual cortex in CBF-weighted fMRI maps obtained before hypercapnia. Since signal change in FAIR was not observed in areas with fast inflowing component (15,20,21), large vessels were not included in the ROI. Within the ROI, BOLD signals originate from capillaries and venous vessels, and nearby tissue. Two images (12.6 sec) at the start of each period of visual stimulation and five images at the start of each period of hypercapnia were excluded from further analysis due to a hemodynamic response delay.

The calibration constant α^* and $CMRO_2$ change were calculated on a ROI basis for quantitative analysis and on a pixel-by-pixel basis for visualization (Fig. 1). Since the *same ROI* for each subject was used for visual stimulation and hypercapnia, CBF and BOLD changes during both conditions were compared directly. Data are presented as means and their standard deviations.

RESULTS

Figure 2 shows a representative result during inhalation of 5% CO_2 gas mixture, which increased the end-tidal pCO_2 level from 4.47 to 5.69 kPa. An anatomic image (Fig. 2A) is a non-slice-selective IR image with an inversion time of 1.4 sec obtained as a part of a FAIR image. The gray matter area has less signal intensity in this T_1-weighted image than the white matter area because T_1s of gray and white matter are 1.0 and 0.7 sec, respectively (33). FAIR (subtraction) images during normocapnia and hypercapnia are shown (Fig. 2B,C). Clearly, in FAIR images, signal intensity is higher in gray than in white matter due to higher CBF and longer T_1 in the gray matter area. CBF-weighted signals increased globally during hypercapnia. Relative CBF and BOLD maps are shown in Fig. 2D and E, respectively. Both CBF, less evident, and BOLD changes were larger in the gray matter than in the white matter. Areas with pronounced BOLD signal change were located at the outer edge of the brain. Relative CBF change within the visual cortex was 44.6% (Fig. 2D), and corresponding BOLD signal change was 3.3% (Fig. 2E) with a gradient echo time of 50 msec. Assuming no $CMRO_2$ change, $\Delta y/(1 - y)$ was 30.8% (step 2). The calibration constant α^* within the visual cortex was 2.17 sec^{-1} using Model 1 and 4.23 sec^{-1} using Model 2 (step 3). Figure 2F shows a map of α^* values using Model 1. A similar spatial distribution of α^* values was observed when Model 2 was used.

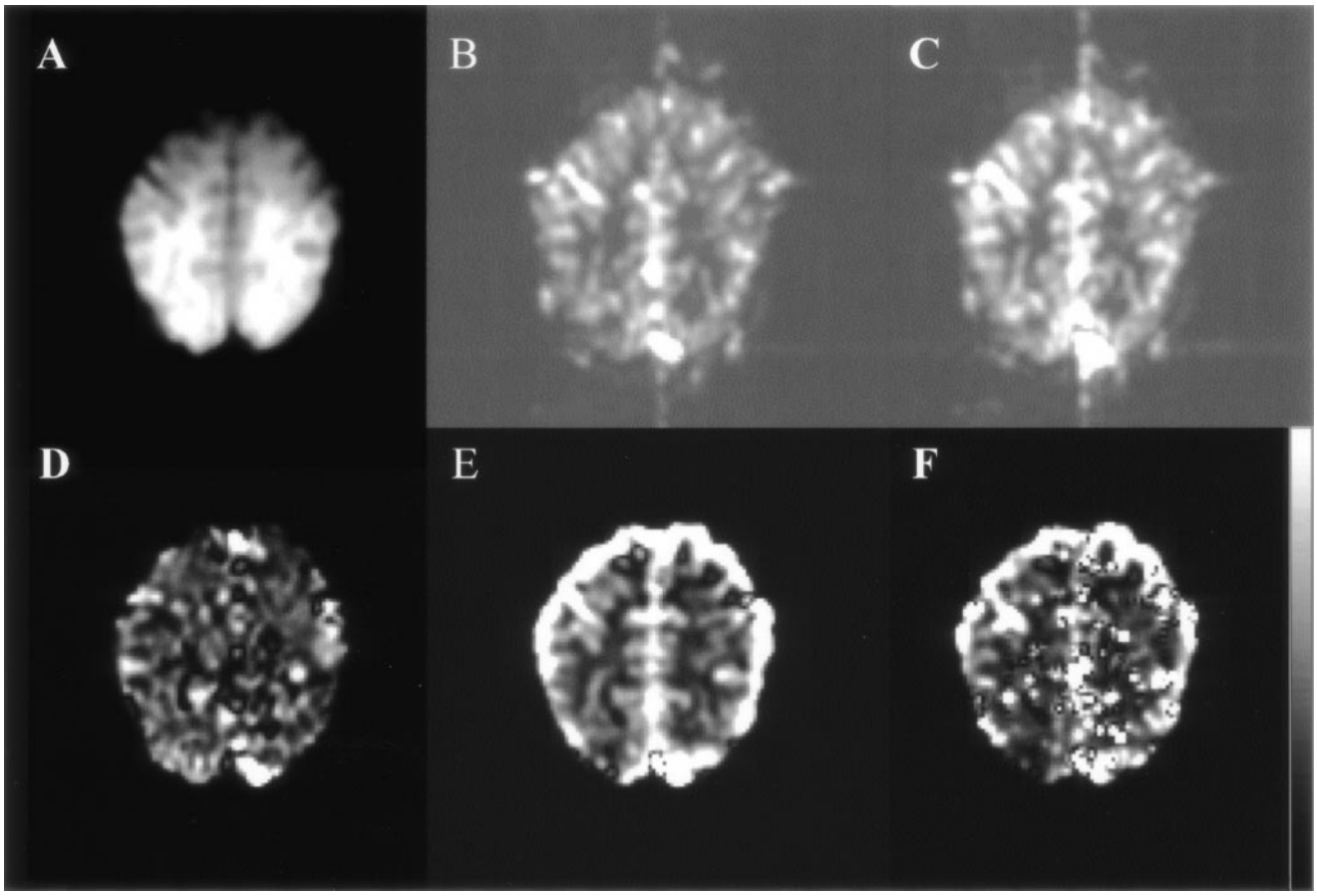

FIG. 2. Representative hypercapnia study of one subject (#4618). **A:** Anatomic image with an inversion recovery time of 1.4 sec, which is a non-slice-selective IR image as a part of the FAIR image. **B** and **C:** CBF-weighted FAIR images during breathing of atmospheric air and 5% CO_2 gas mixture, respectively. Signal intensities in B and C are 20 times less than those in A. **D** and **E:** Relative CBF and BOLD signal changes during hypercapnia, respectively. Gray scale bar ranges from −10% to 100% for CBF and from −1% to 5% for BOLD, respectively. **F:** Calibration constant map of α^* using Model 1. The gray scale bar ranges from −1 to +6 sec^{-1}. For better visualization, smoothing was performed, and a nominal resolution is 1.6 mm.

Average end-tidal pCO_2 levels breathing atmospheric air (normocapnia) and 5% CO_2 gas mixture (hypercapnia) were 4.89 ± 0.45 and 6.35 ± 0.33 kPa ($n = 9$), respectively. The corresponding average CBF and BOLD increases in the visual cortex were 47.3 ± 17.3% and −0.447 ± 0.171 sec^{-1}, respectively (Table 1). Average $\Delta y/(1 - y)$ was 31.3 ± 7.7%. Average α* determined using Model 1 was about half of that determined using Model 2.

In all subjects, CBF increased significantly in the visual cortex during visual stimulation. The average CBF increase within the visual cortex was 43.6 ± 9.4% ($n = 18$), and ΔR_2^* was −0.114 ± 0.086 sec^{-1} ($n = 18$) (Table 1). BOLD and CBF changes measured during visual stimulation *before and after* hypercapnia condition were not significantly different ($P < 0.05$). Except for one subject (#d4887), CBF was highly reproducible for each subject. While CBF increase *during hypercapnia and visual stimulation* was not different, BOLD change was much smaller during neural stimulation than during hypercapnia ($P < 6 \times 10^{-6}$). Two representative fMRI studies during visual stimulation are shown in Fig. 3. CBF, BOLD, and $CMRO_2$ maps were compared using the *same* ROI. The $CMRO_2$ maps were calculated using Model 1 with hypercapnia-calibrated α*. Red color represents high percent change in each physiological parameter. Hot spots of CBF correspond well with those of $CMRO_2$, while hot spots of BOLD are alienated from those of CBF and $CMRO_2$. To compare dynamic responses during hypercapnia and visual stimulation, *averaged* CBF and BOLD time courses of all hypercapnia and visual stimulation studies within visual cortex ROI are shown in Fig. 4.

Individual data of $\Delta f/f$ and ΔR_2^* during hypercapnia and visual stimulation are shown in Table 1 and Figure 5. The calibration constant α* and $\Delta CMRO_2/CMRO_2$ (shown in Table 1) were calculated using both BOLD biophysical models. The relative $CMRO_2$ change calculated using Model 1 was about twice that using Model 2. The relationship between CBF and $CMRO_2$ changes is shown in Figure 6. A weak positive correlation was observed between relative CBF and $CMRO_2$ changes ($r = 0.51$, $P < 0.05$), and a weak negative correlation was observed between BOLD and calculated $CMRO_2$ changes ($r = 0.71$, $P < 0.005$).

DISCUSSION

BOLD and CBF Measurements

We have successfully measured CBF and BOLD changes simultaneously during hypercapnia and visual stimulation. During hypercapnia, the CBF change is consistent with that measured previously using the exact same setup by our group, 58% (26), and agrees well with earlier reported values, 59% by Kety and Schmidt (17), and 40% by Novack et al. (19). The ΔR_2^* change in the gray matter is similar to that measured previously, −0.83 and −0.54 sec^{-1} (26). Spatial distributions of BOLD and CBF signal changes during hypercapnia are not homogenous, similar to that reported by Rostrup et al (26); gray matter area has higher CBF and BOLD changes than white matter. In particular, the outer edge of the brain has a higher BOLD signal change than the inner gray matter area because the surface of the cortex is more likely to have large vascular contributions.

Table 1
CBF, ΔR_2,* and α* During Hypercapnia, and CBF, ΔR_2,* and $CMRO_2$ During Visual Stimulation

Subject ID no.	No. of pixels[1]	Hypercapnia			Visual stimulation[2]		
		CBF (%)	ΔR_2* (sec^{-1})	α* (sec^{-1})[3]	CBF (%)	ΔR_2* (sec^{-1})	$CMRO_2$ (%)[3]
d4616	249	39.0	−0.579	2.13–4.06	41.6	−0.032	39.5–20.5
					49.7	−0.056	45.8–22.9
d4617	164	54.1	−0.564	1.61–3.27	54.1	−0.022	52.0–25.6
					57.8	0.014	59.2–28.6
d4618	235	44.6	−0.668	2.17–4.23	46.2	−0.096	39.7–20.2
					35.9	−0.114	28.8–15.6
d4880	399	25.8	−0.371	1.81–3.25	31.3	−0.079	25.6–13.8
					31.3	−0.159	19.7–10.6
d4881	394	36.2	−0.321	1.21–2.27	39.9	−0.071	31.7–16.5
					32.9	−0.018	31.0–16.7
d4882	263	81.8	−0.210	0.47–1.08	51.0	−0.138	6.3–6.0
					40.3	−0.192	−17.4–−4.0
d4883	321	56.9	−0.504	1.39–2.86	39.1	−0.290	10.1–6.4
					40.0	−0.278	12.0–7.3
d4884	232	29.6	−0.518	2.27–4.15	52.3	−0.068	47.7–23.4
					46.4	−0.200	33.5–16.5
d4887	303	57.6	−0.552	1.51–3.12	62.2	−0.168	44.2–20.8
					32.6	−0.094	24.3–13.6
Mean[4]	284 (78)	47.3 (17.3)	−0.447 (0.171)	1.62 (0.57)–3.14 (1.01)	43.6 (9.4)	−0.114 (0.086)	29.6 (18.8)–15.6 (8.1)

*Nine subjects performed hypercapnia and two visual stimulation studies before and after hypercapnia. All measurements were based on the ROI analysis.

[1]ROI was obtained in the active pixels with significant signal changes of CBF during visual stimulation before hypercapnia.

[2]Two repeated measurements were listed separately for CBF, ΔR_2,* and $CMRO_2$ during visual stimulation. The first row in each subject shows values during stimulation before hypercapnia, and the second row shows those after hypercapnia.

[3]Two BOLD models were used; the first number was obtained using Model 1, and the second number was obtained using Model 2.

[4]Values in parentheses were standard deviations of their means.

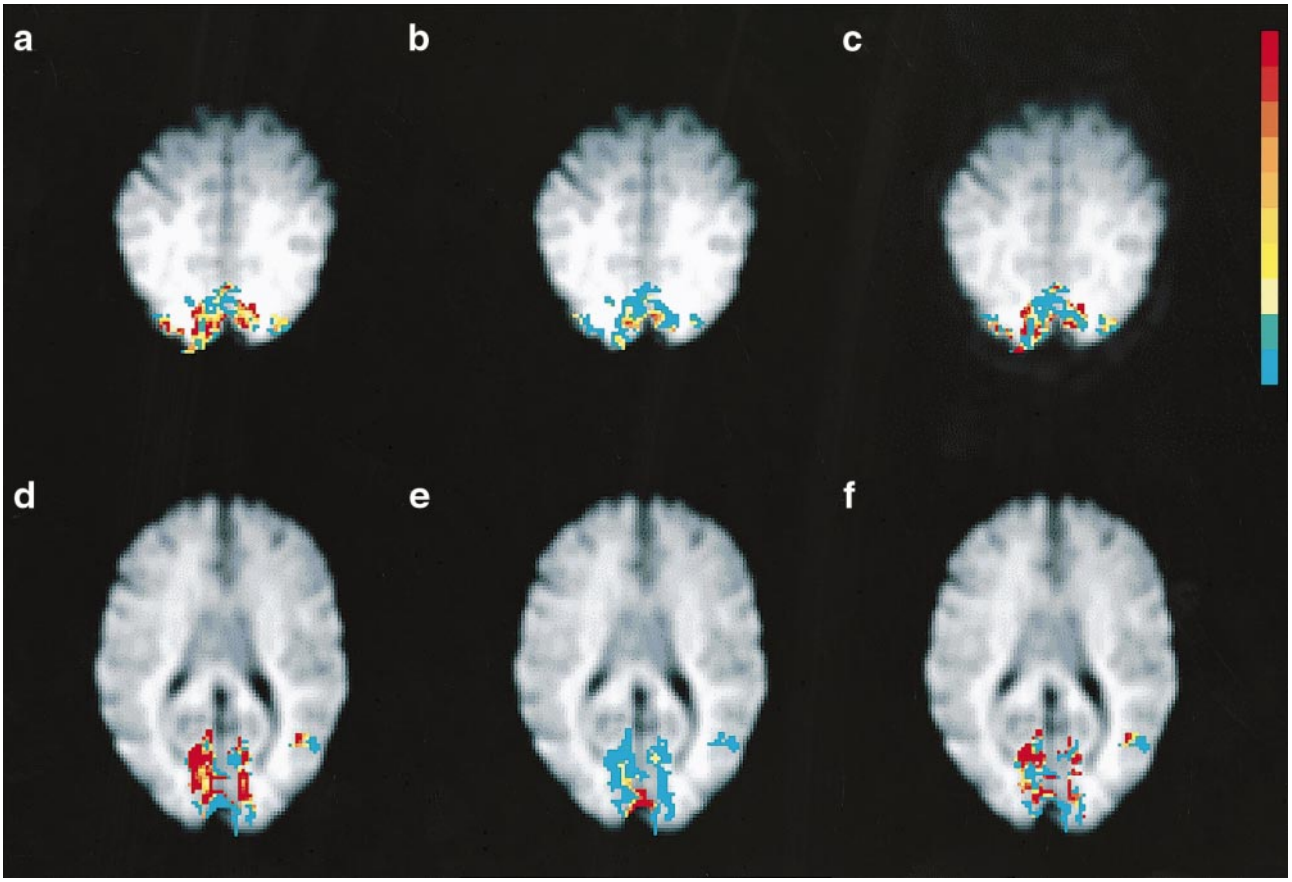

FIG. 3. Representative CBF (**a** and **d**), BOLD (**b** and **e**), and $CMRO_2$ (**c** and **f**) maps of two subjects (abc for subject #d4618 and def for subject #d4883) before hypercapnia. Only active pixels in CBF were used for calculation. Each color represents a 10% increment starting from 30% for CBF and $CMRO_2$ and a 0.15% increment starting from 0.5% for BOLD.

Although a vacuum pillow was employed to minimize head motion, and images were aligned by using motion correction method, the effect of head motion may still contribute to BOLD and CBF. ROI with multiple pixels was less affected by head motion than single pixel, and thus ROI was employed here for quantitative analysis.

During black and white visual stimulation, CBF in the visual cortex increased by 44%, which is consistent with

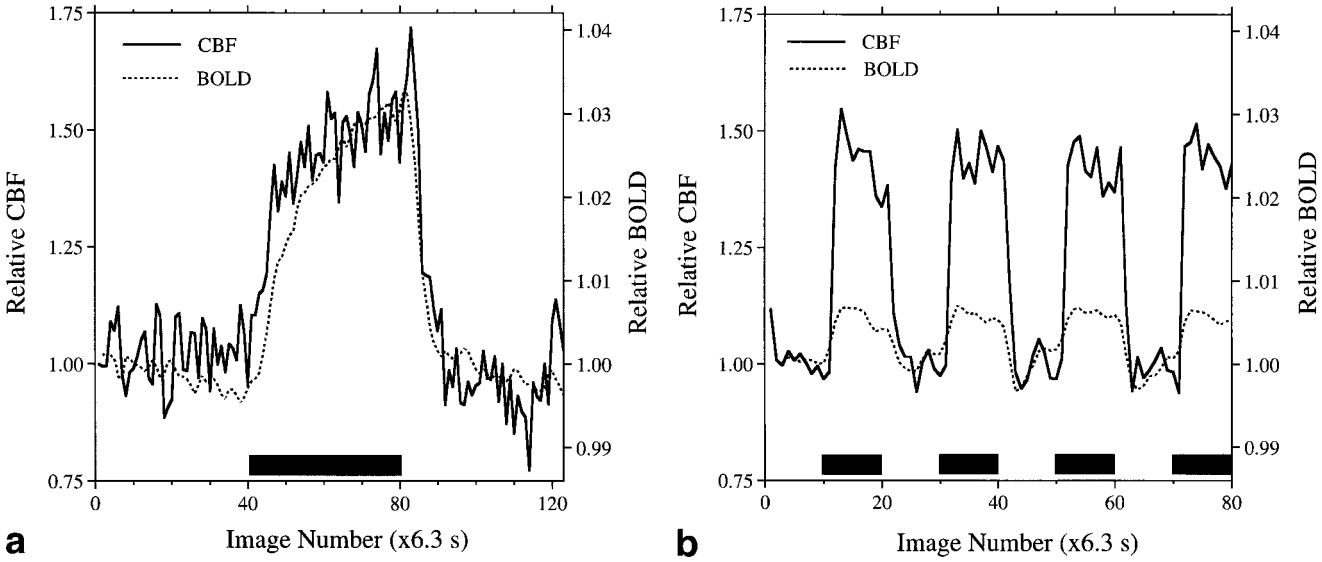

FIG. 4. Averaged time courses of relative CBF and BOLD changes during hypercapnia (**a**) and visual stimulation (**b**). Time courses were obtained by averaging across all subjects. Boxes below time courses indicate hypercapnic (a) and task (b) periods.

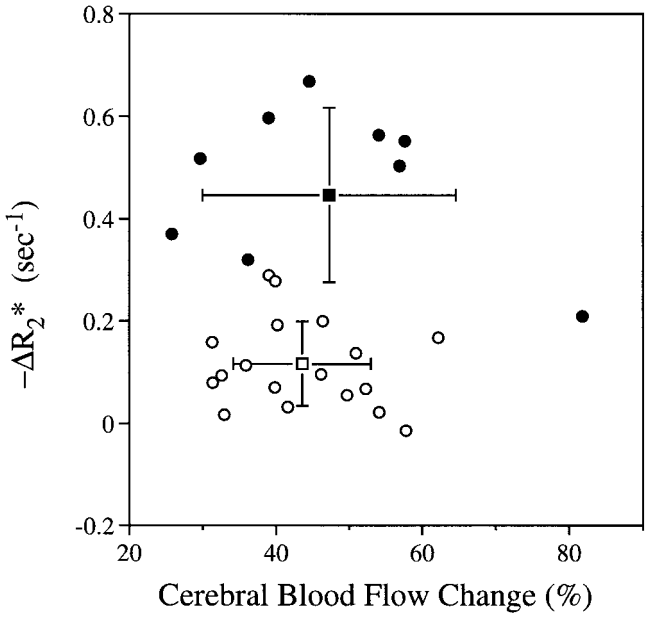

FIG. 5. Plot of ΔR_2^* vs. CBF changes during hypercapnia and visual stimulation. Closed circles correspond to hypercapnia, and open circles represent visual stimulation. Closed and open rectangles represent means of hypercapnia and visual stimulation data, respectively. Bars indicate standard deviations. Individual data points are tabulated in Table 1.

previous PET and fMRI studies using similar paradigms (3,15,16,34). Active pixels in the visual cortex including the primary and associative visual areas from CBF images were used in determining the region of interest for each subject. Average ΔR_2^* was -0.11 sec^{-1}, corresponding to a 0.6% change with a gradient echo time of 50 msec at 1.5 T. This BOLD signal change is lower than values reported by others (6,7). Since we used non-slice-selective IR images with a typical inversion time of 1.4 sec, signal contribution from vessels and CSF was significantly reduced by nulling long T_1 components. We acquired gradient-echo BOLD with and without an inversion pulse in one subject (all other parameters were the same) and found that BOLD without the inversion pulse had a much higher percent change than that with the inversion pulse (data not shown). Thus, suppression of intravascular BOLD component leads to a reduction of the observed signal change in T_1-weighted images. To suppress vascular contributions to BOLD further, bipolar crushing gradients may be used (13,35). Even if vascular contribution is significant, the comparison between BOLD and CBF during hypercapnia and visual stimulation is appropriate because the same ROI and the same imaging sequence were used.

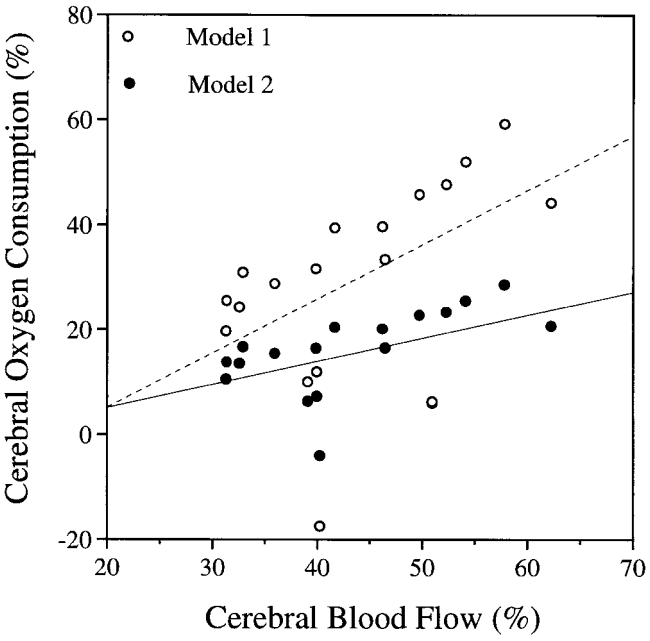

FIG. 6. Relationship between CBF and $CMRO_2$ changes during visual stimulation. Open circles represent data determined from Model 1; closed circles represent data calculated using Model 2. The dashed line is the best fit of open circles; $CMRO_2 = 1.04 \cdot CBF - 15.5$ ($r = 0.52$). The solid line is the best fit of closed circles; $CMRO_2 = 0.44 \cdot CBF - 3.63$ ($r = 0.51$).

The CBF values reported here, measured during hypercapnia and visual stimulation, agree well with those in previous studies (3,15–17,19,26,34). However, the FAIR technique has potential problems for accurate quantification of CBF due to effects of vascular component, mean transit time, and water extraction fraction. Although gradient train in EPI can suppress fast moving components, significant intravascular components will contribute to CBF-weighted MR signals, causing an error in the measurement of relative CBF change (21,36,37). During visual stimulation, mean transit time will shorten due to increase of flow, overestimating relative CBF (24,36). Since water is not freely diffusible at high flow, the water extraction fraction will decrease when CBF increases (37). This effect will underestimate relative CBF change by the ratio of extraction fractions. In our previous animal studies (23), we found that CBF measured by FAIR (without correcting the above-mentioned components) agrees extremely well with that measured using freely diffusible ^{14}C-iodoantypirine at normocapnia and hypercapnia under the same experimental condition in a rat model. This good agreement may occur because the above-mentioned effects cancel out (23,36). Thus, these effects were not included in the calculation of relative CBF. Since relative CBF changes during both hypercapnia and visual stimulation are similar, errors in their quantification will not affect the accuracy of relative $CMRO_2$ calculation.

Recently, it was reported that neural activity-induced CBF response was influenced by hypercapnia, even long after the cessation of hypercapnia; in animal studies during somatosensory stimulation, CBF change was affected by hypercapnia, while BOLD was not affected (38). To examine post-hypercapnia changes in CBF and BOLD, we measured BOLD and CBF changes during visual stimulation before and after hypercapnia condition. The second measurement was performed within 5 min after hypercapnia studies. The BOLD responses before and after hypercapnia were not significantly different. This is also true for CBF. Differences of neural activity-induced CBF responses after hypercapnia between humans and animals may be due to (1) anesthesia used in animal models; (2) different stimulation paradigm; and/or (3) different species.

BOLD Biophysical Model

It was assumed that the major signal sources of BOLD are oxygenation level and blood volume changes. In Eq. [2], a multiplication term of CBV and oxygenation level changes was ignored. In our case, this multiplication term was less than 10% of combined $\Delta y/(1-y)$ and CBV terms. Thus, the approximation is justified. However, if $\Delta y/(1-y) \cdot \Delta\nu/\nu$ term is significant (39), ΔR_2^* should be described by

$$\Delta R_2^* = -\alpha^* \left\{ \frac{\Delta y}{1-y} - \beta^* \frac{\Delta \nu}{\nu} + \kappa \frac{\Delta y}{1-y} \cdot \frac{\Delta \nu}{\nu} \right\}. \qquad [4]$$

The calibration constants can be determined by multiple CBF and BOLD measurements obtained during different hypercapnic (pCO_2) conditions; all three parameters in Eq. [4] can be calculated by a minimum of three independent measurements. If a steady-state condition is achieved during the progress of hypercapnia dynamically in the MRI time domain of seconds, dynamic BOLD and CBF data such as those shown in Fig. 4 can be used to determine the calibration constants. However, in our case, the dynamic data were not well fitted to current BOLD models. Further studies are needed to investigate whether the dynamic data can be utilized for modeling.

In the BOLD model, relative CBV changes play an important role. We derived CBV from CBF using the global relationship in monkeys obtained during hypercapnic conditions. Based on PET studies (see above), this relationship can be applied to regional changes during neural activity. Even if this CBF-CBV relationship is applicable to both global and regional changes, relative CBV change contributing to BOLD is not known. The constant β^* is calibrated with CBV calculated from hypercapnia-induced CBF using Eq. [1]. Then this constant is used for determining BOLD effect contributed from relative CBV change that was calculated from neural activity-induced CBF using Eq. [1]. Thus, the fitted constant will compensate for the error induced by using Eq. [1] as long as CBF and CBV increases have a monotonic relationship within the range of CBF change. It is not critical to use Eq. [1] or other formulae (such as $\Delta\nu/\nu = \gamma \cdot \Delta f/f$) if CBF changes during reference and neural stimulation conditions are comparable.

The constant β^* varies between 0.0 and 1.0. β^* depends on the vessel size, which is closely related to imaging parameters such as gradient echo or spin echo, and magnetic field strength. In the case of $\beta^* = 0.0$, which was obtained from previous measurements (26), the average regional $CMRO_2$ change determined from CBF and BOLD during visual stimulation was 30%, while the CBF change was 44%. In other models, which assumed that CBV contribution is significant (14–16), the calculated $CMRO_2$ is approximately half of the value estimated with Model 1. The accuracy of the calculated $CMRO_2$ change is dependent on that of the calibration constants. Therefore, we calculated the range of relative $CMRO_2$ change, rather than a single value.

No Metabolic Change During Hypercapnia

Another important assumption is that $CMRO_2$ does not change during hypercapnia. In human studies, $CMRO_2$ does not change in mild hypercapnia (up to arterial blood CO_2 tension of 60 mmHg) such as from 43 to 52 mmHg (17), from 40 to 45 mmHg (18), and from 43 to 50 mmHg (19). According to our previous measurements with exactly the same experimental setup, CO_2 tension of arterial blood increased from 41 to 46 mmHg during inhalation of 5% CO_2 (26). In our study we did not measure pCO_2 levels directly from arterial blood, but used end-tidal pCO_2 values obtained via capnometer. End-tidal pCO_2 measurements in the current studies increased from 37 to 48 mmHg. With this small increase of arterial pCO_2 tension during inhalation of 5% CO_2 gas mixture, it is expected that $CMRO_2$ does not change, supporting the validation of the assumption of no metabolic change during hypercapnia.

CBF-CBV Relationship During Hypercapnia and Neural Stimulation

We assumed that CBF-CBV relationships during hypercapnia and neural activity are similar. PET data suggest that the CBF-CBV relationship (Eq. [1]) is similar during hypercapnia and neural activity, as discussed in the Theory section. CBF regulatory mechanisms of both conditions are different, and thus calibration of constants using hypercapnia may not be valid for neural stimulation. However, hypercapnia is so far the only approach for easy modulation of CBF without changing metabolism. If our assumption is not correct and accurate measurement of relative $CMRO_2$ change is not feasible, qualitative comparison is still possible. For example, with similar CBF changes during hypercapnia and visual stimulation, BOLD signal change during neural stimulation was 25% of that during hypercapnia (Figs. 4, 5). This suggests that mismatch of BOLD between hypercapnia and visual stimulation is mainly due to *significant oxygen consumption increase* during visual stimulation.

$CMRO_2$ During Visual Stimulation

We previously proposed the current approach to measure $CMRO_2$ change (15). Initially, we measured BOLD and CBF changes simultaneously during visual stimulation and finger opposition (15,28). Since we did not measure BOLD and CBF during hypercapnia, calibration constant values were based on simulation and physiological data reported in the literature (15,28). Relative $CMRO_2$ changes, 5–8%, calculated by this method were underestimated due to the underestimation of α^*. During the course of our present studies, similar studies of visual stimulation and hypercapnia were performed by others (16). CBF and BOLD signal changes were measured *separately* during visual stimulation at 12 Hz. Calculated $CMRO_2$ increased by 16 ± 2% when β^* was assumed to be 1/1.5 based on simulation, while CBF increased by 45% ($n = 10$). CBF increase was negatively correlated to $CMRO_2$ change ($r = -0.50$). When we set $\beta^* = 1/1.5$ in our data, the resultant $CMRO_2$ increase was 23 ± 9% ($n = 18$). In this report, CBF and BOLD were measured simultaneously, not separately, reducing the experimental time. CBF increase was positively correlated to $CMRO_2$ change, consistent with a conventional concept of coupling between CBF and $CMRO_2$ (8,9,11). Furthermore, visual stimulation was performed before and after hypercapnia, showing that hypercapnia does not affect

post-hypercapnia hemodynamic response during mental activity.

$CMRO_2$ measured by the BOLD/CBF method during black/white visual stimulation increased between 15.6 ± 8.1% and 29.6 ± 18.8% (n = 18). These values are higher than the values measured by Fox et al (3) during red/black circular checker reversing at 10 Hz, and by Ribeiro et al (34) during black/red 8 Hz stimulation using goggles, whereas CBF changes are similar to those obtained in these studies. On the other hand, the ratio of 0.3–0.7 found between $CMRO_2$ and CBF changes agrees well with that determined by Iida et al (40), which was 0.3 in the visual cortex during visual stimulation (40). The wide discrepancy among $CMRO_2$ measurements using PET is partly due to the de-convolution of multiple PET measurements with the usage of different kinetic models. Furthermore, due to technical difficulties, only a few such PET studies have been reported (2,3,9,34). An alternative method is to use NMR spectroscopy measuring turnover of the tricarboxylic acid cycle after injection of ^{13}C-labeled glucose (12). However, spatial resolution of this technique is low. The CBF/BOLD method used here can be used to determine relative $CMRO_2$ changes with high spatial resolution, but may not provide an absolute $CMRO_2$ value. To validate the current method, comparison of relative $CMRO_2$ changes measured by both imaging and PET/NMR spectroscopy methods may be needed.

Although we did use ROI analyses for quantification, it is interesting to compare CBF, BOLD, and $CMRO_2$ maps on a pixel-by-pixel basis. Spatial discrepancy between BOLD and CBF/$CMRO_2$ was observed, which may be due to BOLD dependency on multiple physiological and anatomical parameters including vascular structure. For high spatial resolution studies, BOLD-based fMRI maps with a certain threshold are more likely to contain areas with high percentage change, which may be less active in CBF and $CMRO_2$-based fMRI maps. Since the extent of CBF modulation correlates well with metabolic activity (1), CBF and $CMRO_2$ techniques may provide a reasonably more accurate localization of neuronal activity. Thus, the fMRI method for simultaneous acquisition of CBF and BOLD can be used for either qualitative or quantitative high-resolution studies of CBF and $CMRO_2$.

In summary, we have developed a methodology to measure relative $CMRO_2$ change from BOLD and CBF measurements using hypercapnia as a reference in conjunction with a biophysical model of BOLD. Relative $CMRO_2$ increased significantly during black and white visual stimulation, and its magnitude change was 0.3–0.7 times the CBF change. A weak positive correlation between CBF and $CMRO_2$ changes was observed, suggesting that the $CMRO_2$ increase is proportional to the CBF change.

ACKNOWLEDGMENTS

We thank Karam Sidaros and Irene K. Andersen for helping with the experiments.

REFERENCES

1. Raichle ME. Circulatory and metabolic correlates of brain function in normal humans. In: Handbook of physiology—the nervous system. Bethesda: American Physiological Society; 1987. p 643–674.
2. Fox PT, Raichle ME. Focal physiological uncoupling of cerebral blood flow and oxidative metabolism during somatosensory stimulation in human subjects. Proc Natl Acad Sci USA 1986;83:1140–1144.
3. Fox PT, Raichle ME, Mintun MA, Dence C. Nonoxidative glucose consumption during focal physiologic neural activity. Science 1988;241: 462–464.
4. Ogawa S, Lee T-M, Nayak AS, Glynn P. Oxygenation-sensitive contrast in magnetic resonance image of rodent brain at high magnetic fields. Magn Reson Med 1990;14:68–78.
5. Bandettini PA, Wong EC, Hinks RS, Rikofsky RS, Hyde JS. Time course EPI of human brain function during task activation. Magn Reson Med 1992;25:390–397.
6. Kwong KK, Belliveau JW, Chesler DA, Goldberg IE, Weisskoff RM, Poncelet BP, Kennedy DN, Hoppel BE, Cohen MS, Turner R, Cheng H-M, Brady TJ, Rosen BR. Dynamic magnetic resonance imaging of human brain activity during primary sensory stimulation. Proc Natl Acad Sci USA 1992;89:5675–5679.
7. Ogawa S, Tank DW, Menon R, Ellermann JM, Kim S-G, Merkle H, Ugurbil K. Intrinsic signal changes accompanying sensory stimulation: functional brain mapping with magnetic resonance imaging. Proc Natl Acad Sci USA 1992;89:5951–5955.
8. Buxton RB, Frank LR. A model for the coupling between cerebral blood flow and oxygen metabolism during neural stimulation. J Cereb Blood Flow Metab 1997;17:64–72.
9. Roland PE, Erickson L, Stone-Elander S, Widen L. Does mental activity change the oxidative metabolism of the brain? J Neurosci 1987;7:2373.
10. Marrett S, Fujita H, Meyer E, Ribeiro L, Evans AC, Huwabara H, Giedde A. Stimulus specific increase of oxidative metabolism in human visual cortex. In: Uemura K, et al., editors. Quantification of brain function, tracer kinetics and image analysis in brain PET. New York: Excerpta Medica; 1993. p 217–228.
11. Brodersen P, Paulson OB, Bolwig TG, Rogon ZE, Rafaelson OJ, Lassen NA. Cerebral hyperemia in electrically induced epileptic seizures. Arch Neurol 1973;28:334–348.
12. Hyder F, Rothman DL, Mason GF, Rangarajan A, Behar KL, Shulman RG. Oxidative glucose metabolism in rat brain during single forepaw stimulation: a spatially localized $^{1}H[^{13}C]$ nuclear magnetic resonance study. J Cereb Blood Flow Metab 1997;17:1040–1047.
13. Boxerman JL, Bandettini PA, Kwong KK, Baker JR, Davis TL, Rosen BR, Weisskoff RM. The intravascular contribution to fMRI signal change: Monte Carlo modeling and diffusion-weighted studies in vivo. Magn Reson Med 1995;34:4–10.
14. Ogawa S, Menon RS, Tank DW, Kim S-G, Merkle H, Ellermann JM, Ugurbil K. Functional brain mapping by blood oxygenation level-dependent contrast magnetic resonance imaging. Biophys J 1993;64:800–812.
15. Kim S-G, Ugurbil K. Comparison of blood oxygenation and cerebral blood flow effects in fMRI: estimation of relative oxygen consumption change. Magn Reson Med 1997;38:59–65.
16. Davis TL, Kwong KK, Weisskoff RM, Rosen BR. Calibrated functional MRI: mapping the dynamics of oxidative metabolism. Proc Natl Acad Sci USA 1998;95:1834–1839.
17. Kety SS, Schmidt CF. The effects of altered arterial tensions of carbon dioxide and oxygen on cerebral blood flow and cerebral oxygen consumption of normal young men. J Clin Invest 1948;27:484–491.
18. Hafkenschiel JH, Friedland CK. Physiology of the cerebral circulation in essential hypertension; the effects of inhalation of 5% carbon diaoxide mixtures on cerebral hemodynamics and oxygen metabolism. J Pharmacol Exp Ther 1952;106:391–392.
19. Novack P, Shenkin H, Bortin L, Goluboff B, Soffe AM. The effects of carbon dioxide inhalation upon the cerebral blood flow and cerebral oxygen consumption in vascular disease. J Clin Invest 1953;32:696.
20. Kim S-G. Quantification of relative cerebral blood flow change by flow-sensitive alternating inversion recovery (FAIR) technique: application to functional mapping. Magn Reson Med 1995;34:293–301.
21. Kim S-G, Tsekos NV. Perfusion imaging by a flow-sensitive alternating inversion recovery (FAIR) technique: application to functional mapping. Magn Reson Med 1997;37:425–435.
22. Kwong KK, Chesler DA, Weisskoff RM, Donahue KM, Davis TL, Ostergaard L, Campbell TA, Rosen BR. MR perfusion studies with T1-weighted echo planar imaging. Magn Reson Med 1995;34:878–887.
23. Tsekos NV, Zhang F, Merkle H, Nagayama M, Iadecola C, Kim S-G. Quantitative measurements of cerebral blood flow in rats using the FAIR technique: correlation with previous iodoantipyrine autoradiographic studies. Magn Reson Med 1998;39:564–573.

24. Edelman RR, Siewert B, Darby DG, Thangaraj V, Nobre AC, Mesulam MM, Warach S. Qualitative mapping of cerebral blood flow and functional localization with echo-planar MR imaging and signal targeting with alternating radio frequency. Radiology 1994;192:513–520.
25. Grubb J, Raichle ME, Eichling JO, Ter-Pogossian MM. The effects of changes in $PaCO_2$ on cerebral blood volume, blood flow, and vascular mean transit time. Stroke 1974;5:630–639.
26. Rostrup E, Larsson HBW, Toft PB, Garde K, Thomsen C, Ring P, Sondergaard L, Henriksen O. Functional MRI of CO_2 induced increase in cerebral perfusion. NMR Biomed 1994;7(1/2):29–34.
27. Ogawa S, Lee TM, Barrere B. Sensitivity of magnetic resonance image signals of a rat brain to changes in the cerebral venous blood oxygenation. Magn Reson Med 1993;29:205–210.
28. Kim S-G, Tsekos NV, Ashe J. Multi-slice perfusion-based functional MRI using the FAIR technique: comparison of CBF and BOLD effects. NMR Biomed 1997;10:191–196.
29. Woods RP, Cherry SR, Mazziotta JC. Rapid automated algorithm for aligning and re-slicing PET images. J Comput Assist Tomogr 1992;16: 620–633.
30. Bandettini PA, Jesmanowicz A, Wang EC, Hyde JS. Processing strategies for time-course data sets in functional MRI of human brain. Magn Reson Med 1993;30:161.
31. Forman SD, Cohen JD, Fitzgerald M, Eddy WF, Mintun MA, Noll C. Improved assessment of significant activation in functional magnetic resonance imaging (fMRI): use of a cluster-size threshold. Magn Reson Med 1995;33:636–647.
32. Xiong J, Gao JH, Lancaster JL, Fox PT. Clustered pixels analysis for functional MRI activation studies of the human brain. Hum Brain Map 1995;3:287–301.
33. Breger RK, Rimm AA, Fischer ME, Papke RA, Haughten VM. T_1 and T_2 measurements on a 1.5 Tesla commercial imager. Radiology 1989;171: 273–276.
34. Ribeiro L, Kuwabara H, Meyer E, Fujita H, Marrett S, Evans A, Gjegge A. Cerebral blood flow and metabolism during nonspecific bilateral visual stimulation in normal subjects. In: Uemura et al., editors. Quantification of brain function in tracer kinetics and image analysis in brain PET. Amsterdam: Elsevier Science; 1993. p 229–236.
35. Song AW, Wong EC, Tan SG, Hyde JS. Diffusion-weighted fMRI at 1.5T. Magn Reson Med 1996;35:155–158.
36. Ye FQ, Mattay VS, Jezzard P, Frank JA, Weinberger DR, McLaughlin AC. Correction for vascular artifacts in cerebral blood flow values by using arterial spin tagging techniques. Magn Reson Med 1997;37:226–235.
37. Silva AC, Zhang W, Williams DS, Koretsky AP. Estimation of water extraction fractions in rat brain using magnetic resonance measurement of perfusion with arterial spin labeling. Magn Reson Med 1997;37: 58–68.
38. Bock C, Schmitz B, Kerskens CM, Gyngell ML, Hossman H-A, Hoehn-Berlage M. Functional MRI of somatosensory activation in rat: effect of hypercapnic up-regulation on perfusion- and BOLD-imaging. Magn Reson Med 1998;39:457–461.
39. Ogawa S, Menon RS, Kim S-G, Ugurbil K. On the characteristics of functional magnetic resonance imaging of the brain. Annu Rev Biophys Biomol Struct 1998;27:447–474.
40. Iida H, Kanno I, Miura S. Rapid measurement of cerebral blood flow with positron emission tomography. New York: Wiley; 1991. p 23–42.